Metal sulfide sub-nanometer clusters formed within calix(8)arene Langmuir-Blodgett films

OZKAYA, Cansu, ABU-ALI, Hisham, NABOK, Alexei <http://orcid.org/0000-0002-9078-1757>, DAVIS, Frank, WALCH, Nik, HAMMOND, Deborah and CAPAN, Rifat

Published version

OZKAYA, Cansu, ABU-ALI, Hisham, NABOK, Alexei, DAVIS, Frank, WALCH, Nik, HAMMOND, Deborah and CAPAN, Rifat (2023). Metal sulfide sub-nanometer clusters formed within calix(8)arene Langmuir-Blodgett films. Thin Solid Films, 782: 140024.

Thin Solid Films 782 (2023) 140024

Contents lists available at ScienceDirect

Thin Solid Films

journal homepage: www.elsevier.com/locate/tsf

Metal sulfide sub-nanometer clusters formed within calix(8)arene Langmuir-Blodgett films

Cansu Ozkaya [a], Hisham Abu-Ali [b,d], Alexei Nabok [b,*], Frank Davis [b], Nik Walch [b], Deborah Hammond [c], Rifat Capan [a]

[a] Balikesir University, Physics Department, Turkey
[b] Sheffield Hallam University, Materials Engineering Research Institute, Sheffield, UK
[c] The University of Sheffield, Department of Chemistry, Sheffield, UK
[d] University of Basrah, College of Science, Biology Department, Basrah, Iraq

ARTICLE INFO

Keywords:
Langmuir Blodgett films
Calixarenes
Metal sulfides
II-VI semiconductors
Nanoparticles
Size quantization
Energy bandgap

ABSTRACT

This work describes the construction of layered Langmuir-Blodgett (LB) films of a calixarene and the use of these as matrices for the synthesis of a range of metal sulfide nanoparticles. CuS, CdS, HgS, and PbS nano-clusters were formed within LB films of an octa-tertbutyl-calix(8)arene substituted with carboxylic acid groups deposited on different substrates (glass, quartz, and silicon) from either: (i) aqueous sub-phases containing 0.5 mM of the respective metal chloride salt (e.g. $CuCl_2$, $CdCl_2$, $HgCl_2$, $PbCl_2$), or (ii) by soaking the LB films in 10 mM solutions of the above salts for 1 h. The formation of metal-sulfide (MeS) nanoparticles was then achieved by exposing samples to H_2S gas for 10–12 h.

Deposition from salt containing subphases was more reliable and resulted in stoichiometric metal sulfides (CdS, HgS, PbS) being formed within LB films of the calix(8)arene carboxylic acid whereas Cu tended to form polysulfides. UV–vis absorption spectroscopy showed the presence of multiple absorption bands corresponding to electron transitions between energy levels in nanoclusters formed as result of quantum confinement of electrons and holes. The MeS clusters obtained by this process are amongst the smallest reported for LB films, being of the range 0.6–1.2 nm.

1. Introduction

Metal-sulfide semiconductor materials have been widely studied for many years. As their particle sizes grow smaller, into the nanomaterial range, the particle size begins to exert major effects on the behavior of the material. Size-quantization in II-VI semiconductors is a known phenomenon where the adsorption spectra and exciton energy spectra are affected by quantum confinement of free carriers within nano-particles [1] as well as affecting electronic properties (excited states, ionization potential, electron affinity) of the semiconductors [2]. The interest in nano-particulate II-VI semiconductors has been revived recently due to a variety of possible applications in electronics (LEDs) and biosensing (luminescent labels).

One method of generating thin films of metal sulfide materials is to deposit ordered thin films of organic molecules using the Langmuir-Blodgett (LB) technique and then carry out chemical reactions within this matrix to generate the desired nanoparticles. In early works, amphiphilic molecules such as stearic acid were used for deposition of LB films from aqueous subphases containing metal salts, and then the resultant metal stearate films were exposed to H_2S gas causing regeneration of stearic acid and generation of metal sulfides [3]. Copper stearate proved to be too rigid to be deposited as an LB film, however stearic acid could be deposited from a water subphase and the resulting film treated with aqueous copper chloride to generate an LB film of copper stearate [4]. Exposure of this film to H_2S led to generation of a range of copper sulfide nanoparticles, the composition of which was dependent on the pressure of the H_2S used. Similar methods were used to generate CdS and HgS inside LB films of stearic or behenic acid [5]. Cadmium arachidate could also be used to generate CdS, with a thickness increase of about 0.3 nm per layer as shown by ellipsometry [6]. The resulting CdS was thought to exist as approximately 5 nm particles or disk-like plates.

Other researchers used a stepwise method where cadmium stearate LB films were exposed to H_2S to generate CdS nanoparticles, the

* Corresponding author.
E-mail address: a.nabok@shu.ac.uk (A. Nabok).

https://doi.org/10.1016/j.tsf.2023.140024
Received 30 April 2023; Received in revised form 18 August 2023; Accepted 19 August 2023
Available online 22 August 2023

resulting composite could then be immersed in $CdCl_2$ solution and re-exposed to the gas [7]. This allowed more and more CdS to be incorporated into the film and increased the size of the CdS particles, with an increase in film layer spacing from 5.00 nm to 5.09 nm and 5.23 nm after two sulfidation cycles as shown by X-ray diffraction. Further work showed the layer structure of the film could be disrupted but not completely destroyed by this process, leading the authors to propose formation of a CdS plane within the film [8].

Other research groups used a long-chain acid containing a diacetylene moiety as a host for the growth of CdS, CdSe and CdTe [9]. The sizes of the nanoparticles were estimated to be about 5 nm and were thought to be disk-like in nature. Polymerization of the diacetylene was unaffected by the presence of the chalcogenides. Diluting the cadmium levels in the film by mixing it with calcium ions had no effect on particle size, but the size of CdS in the films could be reduced by using mixed fatty acid/cationic surfactant LB films as the host. Mixed chalcogenide particles could be synthesized by exposing CdS containing films to H_2Se or H_2Te.

A range of amphiphiles including stearic acid, fatty acids containing fluorinated chains or azobenzene units and a phosphonic acid, all with differing surface areas could be deposited as LB films and used as hosts for the growth of CdS [10]. The size of the CdS clusters was dependent on both the area per molecule of the host acid and the number of sulfidation steps. Stearic acid was also used as a host for forming PbS and ZnS and stepwise growth. Copper stearate was unsuitable for deposition, so n-octadecyl acetoacetate was used and copper sulfide, probably Cu_2S, was synthesized. When a CdS containing film was treated with lead containing solution and H_2S, it appeared that PbS deposited as a layer on the CdS to give core-shell particles [11]. This was expanded by making bimetallic systems where zinc and lead could be deposited onto CdS in stearic acid LB films to give ZnS-CdS and PbS-CdS core-shell particles [12]. The reverse systems proved impossible since cadmium displaced the zinc and lead from their respective sulfides. However, mixing the metal ions together within the films before sulfidation led to mixed metal sulfides. Similarly, films containing HgS could be treated with cadmium and H_2S to give core-shell particles, however when CdS was treated with Hg salts and H_2S, the mercury ions were found to diffuse into the CdS particles to give highly fluorescent mixed systems [13].

Calixarenes are a range of cyclic phenol-formaldehyde oligomers which have been shown to form good quality LB films [14] and to form films capable of binding a wide range of ions [15]. One issue with using relatively low molecular weight fatty acids as a matrix for the formation of metal sulfides is that they can be fragile, and their structure disrupted by chemical reactions. Since calixarenes have much higher molecular weights, they could be more robust, and also their inherent cyclic structures and porous nature may enable them to act as a template for the formation of ultra-small nanoparticles. Calix(4 and 8)arenes could be deposited from cadmium containing subphases and treated with H_2S to give CdS particles. XPS showed the formation of CdS nanoparticles, and the UV spectroscopy study gave their diameters to be about 1.5 ± 0.3 nm [16]. The calixarene size did not appear to affect the particle size, although larger particles were formed when the pH of the subphase was increased, due to increased ionization of the carboxylate groups leading to enhanced uptake of metal ions and resulting in more CdS being formed within the LB films. Low angle X-ray diffraction and ellipsometry showed no noticeable changes in film order and thickness for calixarene films after CdS generation [17] although under our conditions, cadmium stearate films gave much larger (3–5 nm) particles and lost their ordered layer structure upon sulfidation. Further work utilizing calixarenes with different ring sizes and sidechain lengths [17], again showed only minimal effects of calixarene matrices on the CdS formed. The CdS showed an increase in its first exciton transition to 3.2 eV compared to 2.7 eV for CdS in stearic acid films [18]. TEM studies proved the formation of CdS nanoclusters within the calixarene LB film matrices [18], while electron diffraction showed the CdS to have a zinc blende type structure rather than a wurtzite structure typical for bulk CdS [18].

Within this work we have extended our previous studies on cadmium containing calixarene LB films using a variety of bivalent metals, i.e. Cu, Cd, Hg, and Pb. We investigated the effects of metal salts on the monolayer and deposition behavior of the calix(8)arene and demonstrated the formation of MeS materials within these matrices using X-ray photoelectron spectroscopy (XPS). The formation of metal sulfide nanoclusters within calix(8)arene LB film matrices were confirmed by UV–vis absorption spectroscopy and ellipsometry studies; the calculations of bandgap energies and nanoparticles sizes were made using the theory of quantum confinement.

2. Materials and methods

The chemical structure of octa-tertbutyl-calix(8)arene substituted with carboxylic acid used in this work is shown as inset in Fig. 1. The synthesis of the carboxylic acid substituted calix(8)arene has been previously described [14]. Chloroform, isopropanol and the metal dichloride salts of cadmium, copper, lead and mercury were purchased from Sigma-Aldrich and used without further treatment. Surface pressure-area isotherms and LB deposition were carried out using a NIMA 622 LB trough. The calix(8)arene was dissolved in chloroform (0.2 mg/ml) and spread on a subphase of water or aqueous subphases containing metal chloride salts ($CuCl_2$, $CdCl_2$, $HgCl_2$, $PbCl_2$) in 0.5 mM concentrations since previous work showed good deposition from this concentration for $CdCl_2$ [16–18]. Deionized water with resistivity higher than 15 MΩ·cm was used for preparation of metal salt solutions as well as a subphase. Substrates for LB deposition (i. e. glass, quartz, silicon) were cleaned extensively with water, isopropanol, and chloroform before use.

LB depositions were carried out at a surface pressure of 20 mN/m and a speed of 10 mm/min on different substrates, e. g. glass, quartz, and silicon. Using aqueous salt subphases allowed the uptake of metal ions into calix(8)arene LB films as demonstrated before [14–16], alternatively the LB films could be deposited from pure water subphases and then metal ions incorporated by soaking the LB films in a 10 mM salt solution for 1 hour. LB films of metal- containing calix(8)arene were then placed in a sealed container and exposed to H_2S (which was generated by adding dilute HCl to solid Na_2S) for 10–12 h.

Ellipsometry measurements of LB films deposited on pieces of Si wafer were carried out using J.A. Woollam M2000 spectroscopic instrument at 70° incidence. UV–vis absorption spectra were recorded on LB films deposited on quartz substrates using a Carry 50 (Varian) spectrophotometer. X-ray photoelectron spectroscopy (XPS) measurements were carried out using a Kratos Supra instrument with a monochromatic aluminum X-ray source. Survey scans were collected between 1200 and 0 eV binding energy, at 160 eV pass energy with 1 eV intervals and 300 s/sweep.

3. Results and discussion

3.1. Surface pressure vs area isotherms

Fig. 1 shows the surface pressure-area (Π-A) isotherms of calix(8)arene on water and salt subphases recorded at a constant compression rate of 50 cm^2/min. On pure water subphase, the surface pressure of the calix(8)arene increased until a collapse pressure of approximately 30 mN/m was reached. The values of the area per molecule (estimated by extrapolation of the linear sections of isotherms) varied from 205 to 230 $Å^2$ and are consistent with the values reported earlier [16–18], and the size of ttb-Calix(8)arene-OCH_2COOH molecules as determined by CPK models. The addition of the metals salts in all cases led to an increase in surface area with cadmium having the smallest effect and lead the largest; this is probably a combination of ionic size, possible changes in calix conformation and charge repulsion. Use of metal salts also caused increases in collapse pressure compared to the monolayer spread on

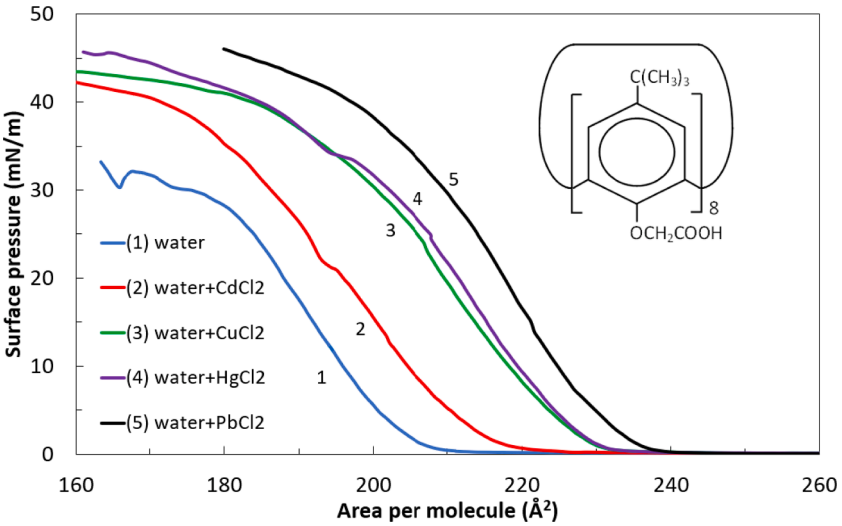

Fig. 1. Surface pressure -area isotherms of the calix(8)arene on water (1) and subphases containing 0.5 mM metal chlorides (2–5). Inset shows the chemical structure of octa-tertbutyl-calix(8)arene carboxylic acid.

pure water.

The values of compressibility modulus (C_s^{-1}) for the monolayers of calix[8]arene spread on different subphases were evaluated at the middle of the linear sections of Π-A isotherms using a formula described lately in [19]:

$$C_S^{-1}(mN/m) = -A\left(\frac{d\Pi}{dA}\right), \quad (1)$$

where $\frac{d\Pi}{dA}$ is the gradient of the linear section of Π-A isotherm and A is the area per molecule at the middle of the isotherm linear section. The values of $d\Pi/dA$ are very similar upon all subphases used and equal to 1.21±0.08 mN/m per Å^2; this is a clear indication of a common nature of interaction between calixarene moieties upon compression. The estimated values ofC_S^{-1} vary slightly from 230 mN/m to 270 mN/m (depending on the subphase used) and correspond to the LC (liquid-condensed) state of monolayers of amphiphilic molecules on aqueous subphases [19].

The different metal ions do lead to different collapse pressures and surface areas, there could be a number of reasons for this such as the differing sizes of the ions and their affinities to the -COOH groups. There could also be differing levels of uptake of the metal ions into the monolayer. At the air-water interface a number of the -COOH groups will dissociate to -COO$^-$ and form salts with the metal ions in the subphase. The ratio of these two species will vary depending on the pH as has been shown by previous work where the amount of CdS formed in the calix LB film increased with the pH [16]. If we assume that each metal ion is bound to two carboxylate groups, our XPS results indicate that between 50% ($HgCl_2$ subphase) up to 80% ($PbCl_2$ subphase) of -COOH groups have dissociated. Other work on mixed LB films including calixarene acids has shown by FTIR studies that both -COOH and -COO$^-$ groups coexist within the LB film [20].

3.2. LB deposition from pure water subphases

Since the incorporation of metal ions in the subphase obviously affects the monolayer structure, it was initially hoped that it would prove possible to deposit the calixarene from a pure water surface and then diffuse in metal ions from solution since this would mean that all the LB films would have identical structures, before modification with metal ions and then hydrogen sulfide. Initial studies were made using calix(8) arene deposited at a surface pressure of 20 mN/m onto glass and silicon. Although the monolayer was stable at these pressures, the deposition proved to be problematic. A good deposition was observed on upstrokes (Z-type deposition), while only minimal deposition occurred on downstrokes; in some cases the deposited film peeled off from the substrate onto the water surface. Increasing surface pressure had no effect on deposition and if too high caused monolayer collapse, whereas reducing the pressure to 15 mN/m lead to the film failing to transfer on upstrokes.

At 20 mN/m it proved possible to construct films with a thickness of 20 layers. The films deposited were soaked in 10 mM salt solutions for 1 hour to incorporate metal ions into the films. Then the films were treated with H_2S to form metal sulfides within the films.

3.3. Deposition from the subphase containing metal salts

Because of the irregular transfer of calix(8)arene from water surfaces, attempts were made to incorporate the metal ions by depositing the calixarene from a subphase containing the metal chlorides. At 20 mN/m, good reproducible Y-type deposition was observed with transfer ratios very close to one for cadmium, copper and lead containing subphases. Films of 40 layers thick could be built up easily with no signs of deposition failing or films peeling off the substrate. When mercury salts were included in the subphase, Y-type deposition was obtained but with a lower transfer ratio of 0.7. This could indicate either incomplete transfer or alternatively a rearrangement of the calix structure upon deposition. Increasing surface pressure led to slow monolayer collapse. All the resultant films were then treated with H_2S gas.

3.4. Spectroscopic ellipsometry study

Spectroscopic ellipsometry measurements were carried out on samples of LB films deposited on pieces of silicon wafer after every stage of treatment, e. g. as deposited, after soaking in metal chloride salts (for films deposited from water subphase) and after treatment in H_2S gas. Fig. 2 shows typical spectra of Ψ and Δ for samples of calix(8)arene LB films (20 layers) deposited from a water sub-phase on silicon, then treated with $PbCl_2$ salt solution, then exposed to H_2S. Judging from the shapes of the spectra and the values of Ψ and Δ the films are fairly thin (in the range of tens of nanometres); small changes in Ψ spectra indicate similar values of refractive index while the decrease in Δ means increases in the film thickness. More accurate evaluation of the values of thickness (d) and refractive index (n) for all samples was achieved by data fitting using the Cauchy dispersion function for refractive index of transparent dielectric films:

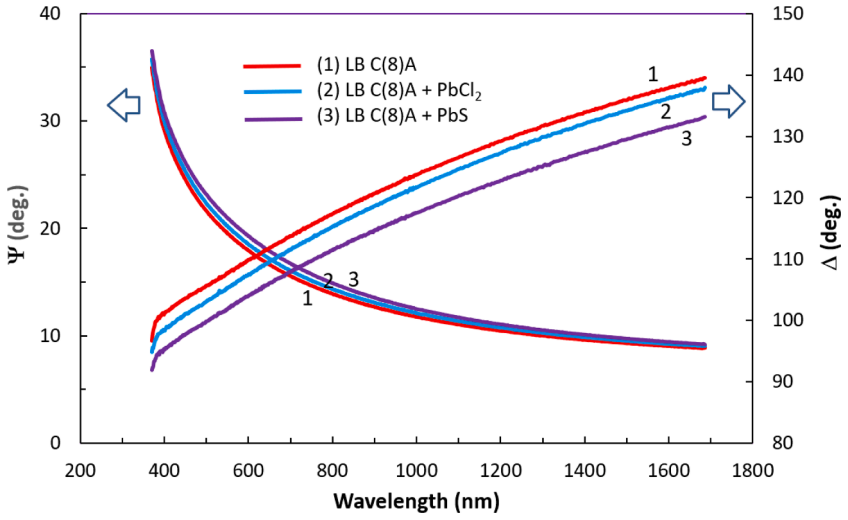

Fig. 2. Typical ellipsometry spectra of Ψ (left axis) and Δ (right axis) for a 20 layer calix(8)arene LB film as deposited on Si-wafer (1), after soaking it in $PbCl_2$ aqueous solution (2) and then after exposure to H_2S gas (3).

$$n = A + B/l^2 + C/l^4,\ k = 0, \quad (2)$$

Zero value for extinction coefficient (*k*) was chosen because the LB films were almost transparent in the ellipsometry spectral range of 370–1680 nm. The obtained values of *d* and Cauchy dispersion parameters *A* and *B* as well as *n* at a fixed wavelength of 633 nm are given in Table 1. The differences in thicknesses of the untreated films are probably due to the irregularities in LB deposition.

As can be seen, in the first series (Table 1a) of samples made by soaking calix(8)arene in solutions of the salts followed by H_2S treatment, both the thickness and refractive index change upon formation of MeS (where Me represents the metal atom) because of incorporation of metal sulfide nanoparticles in the film. Exposure to metals salts led to no or small increases in thickness and changes in refractive index. Calix(8)arenes contain internal cavities and form porous films so incorporating metal ions can occur without major changes in thickness. The formation of MeS nano-clusters caused increases in both the film thickness (except for Cd) and decreases in refractive index (except for Cu).

The second group of samples (Table 1b) where the calix(8)arene was deposited from subphases containing cadmium, copper, mercury or lead salts showed thicknesses twice that of the first group, consistent with their Y-type deposition occurring on both down- and up- strokes, in contrast the films deposited from pure water subphases where deposition only occurred on upstrokes only (Z-type). Films obtained from mercury-containing subphases were noticeably thinner, consistent with the lower level of deposition for these systems. Calix(8)arene LB films produced from $MeCl_2$ sub-phases followed by H_2S treatment, already had metals inserted into calixarene cavity, thus both the thickness and refractive index do not change substantially which has been confirmed earlier by X-ray reflectometry of calix(8)arene/CdS films [17]. However, slight increases in the refractive index of calix(8)arene LB films may indicate the formation of metal sulfide clusters.

Table 1
Ellipsometry data for the calix(8)arene LB films soaked in metal salts (a) and deposited from subphases containing metal salts (b).

(a) Materials	d (nm)	d (nm/ layer)	A	B	n at 633 nm)
C[8]A	28.00	2.800	1.521	0.01	1.546
C[8]A soaked in $CuCl_2$	28.00	2.800	1.523	0.01	1.548
C[8]A+CuS	33.29	3.329	1.538	0.003	1.547
C[8]A	32.30	3.230	1.514	0.01	1.539
C[8]A soaked in $CdCl_2$	33.23	3.323	1.517	0.01	1.542
C[8]A+CdS	32.97	3.297	1.498	0.004	1.508
C[8]A	28.93	2.893	1.533	0.01	1.558
C[8]A soaked in $HgCl_2$	31.01	3.101	1.541	0.01	1.566
C[8]A+HgS	36.62	3.662	1.489	0.01	1.514
C[8]A	26.16	2.616	1.542	0.01	1.567
C[8]A soaked in $PbCl_2$	27.64	2.764	1.554	0.01	1.579
C[8]A+PbS	34.18	3.418	1.513	0.005	1.525
(b) Materials	***d* (nm)**	***d* (nm/ layer)**	***A***	***B***	***n* at** 633 nm)
C[8]A from $CuCl_2$ subphase	65.11	3.26	1.577	0.01	1.602
C[8]A+CuS	64.24	3.21	1.651	0.01	1.637
C[8]A from $CdCl_2$ subphase	59.34	2.97	1.525	0.01	1.550
C[8]A+CdS	61.17	3.06	1.549	0.01	1.574
C[8]A from $HgCl_2$ subphase	38.43	1.92	1.441	0.01	1.466
C[8]A+HgS	43.15	2.16	1.443	0.01	1.468
C[8]A from $PbCl_2$ subphase	62.55	3.13	1.584	0.01	1.609
C[8]A+PbS	61.25	3.06	1.612	0.01	1.637

3.5. UV/Vis spectroscopy study of LB films

Although our UV/Vis results demonstrated formation of MeS materials inside LB films deposited from water or aqueous salt substrates, we report results for films deposited from salt solutions since the films were thicker and of better quality and reproducibility.

Typical UV–vis absorption spectra of an LB film deposited from a PbS containing subphase onto a quartz substrate before (curve 1) and after (curve 2) H_2S treatment are shown in Fig. 3. Because the changes in the spectra caused by the formation of MeS nanoclusters are very small, the true spectra of MeS nanoclusters (curve 3 in Fig. 3) were obtained by subtraction of spectra recorded on LB films before and after treatment with H_2S gas. In order to evaluate the energy band gaps of the MeS semiconductors, the resulted spectra were presented as Abs^2 vs the quantum energy hν (eV) in Fig. 4. The values of E_g were found by linear approximation of the adsorption band edge as shown in Fig. 4.

An estimate of the MeS cluster size can be made from the blue spectral shift caused by quantum confinement of excitons within MeS clusters. The obtained values of E_g found from the respective absorption band edges in Fig. 4 are summarized in Table 2 and appeared to be shifted to higher energy as compared to the corresponding E_g values for the bulk materials. Such an effect can be explained by quantum confinement of electrons and holes in small semiconductor clusters. The

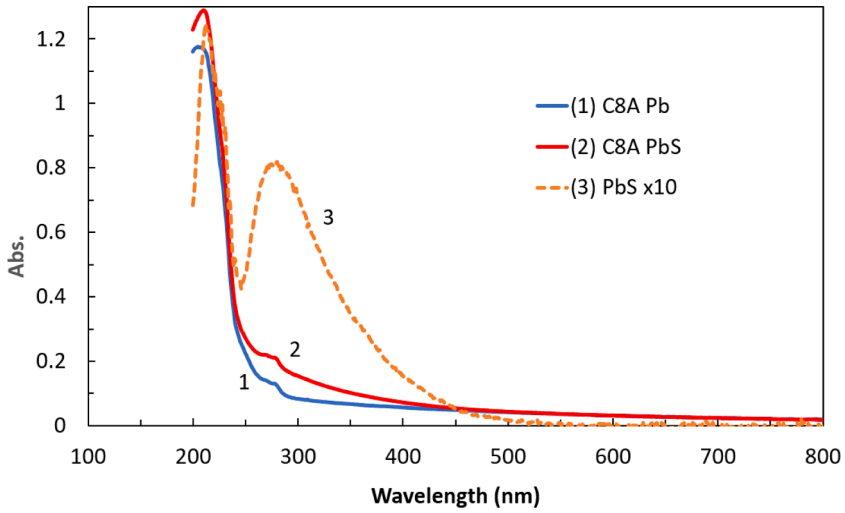

Fig. 3. Typical example of UV–vis absorption spectra of calix(8)arene LB film (40 layers) deposited from the aqueous sub-phase containing $PbCl_2$ before and after H_2S treatment (a) and the resulting spectrum of PbS (Abs. values multiplied by 10) (b).

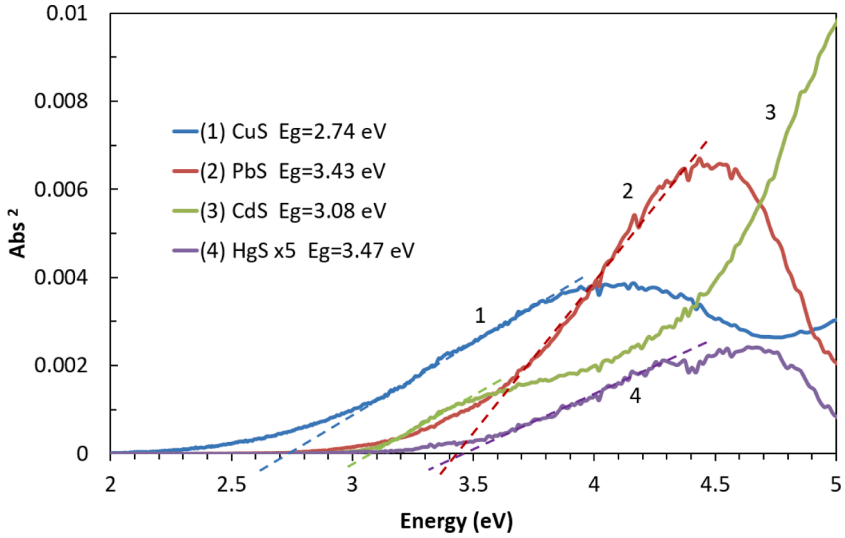

Fig. 4. UV/Vis spectra of metal sulfide formed within C[8]A LB films (40 layers) presented as Abs^2 vs the quantum energy hν (eV):CuS (1), PbS (2), CdS (3) and HgS (4). The values of Eg were found by linear approximation of the adsorption band edges.

Table 2
Estimation of the MeS cluster size from the blue spectral shift caused by quantum confinement.

Material	Eg (eV)	Eg bulk (eV)	ΔE (eV)	*a* (nm)
CuS	2.74	1.55	1.19	1.0
CdS	3.08	2.42	0.68	1.2
HgS	3.47	2.1	1.26	1.1
PbS	3.43	0.37	3.06	0.6

size of a cluster can be estimated from the spectral shift (ΔE) using the Lifshiz-Slezov model [21].

$$\Delta E = \frac{\hbar^2 \pi^2}{2Ma^2} \tag{3}$$

where $M = m_e^* + m_h^*$ is the exciton mass equal to a sum of effective masses of electrons (m_e^*) and holes (m_h^*), a is a nanoparticle diameter. The sizes of MeS clusters appeared to be in the range from 0.6 to 1.2 nm, which corresponds well to the size of the calix(8)arene cavity of about 1.6 to 1.7 nm in diameter and is consistent with the hypothesis of the MeS clusters being embedded inside the calixarene cavities [16]. Such nano-clusters are amongst the smallest obtained for LB films, possibly arising as a combination of restricted diffusion within the robust calix(8) arene films and a templating effect of the macrocyclic host.

There are several interactions that may template the formation of metal sulfide within the calixarene pore. The initial interaction is the electrostatic interaction between metal and carboxylate, locating the metal ions in the vicinity of the calixarene lower rim. As the reaction with H_2S progresses and the nanoparticles form, there is potential for them to migrate into the calixarene cavity, thereby limiting their growth. Besides electrostatic interactions, the electron rich aromatic regions of calixarenes have been shown to readily interact with large metal ions, for example a caesium/p-tert-butylcalix(4)arene salt was shown by X-ray crystallography to have a structure where the caesium atom, instead of being located in the vicinity of the hydroxyl groups, was bound within the calix(4)arene cavity [22]. Similar interactions could potentially occur between the electron-rich calixarene aromatic rings and the metal ions used in this study.

All the spectra of MeS nano-clusters embedded in calix(8)arene LB films show multiple absorption bands which could be found by spectra

de-convolution as shown in Fig. 5. These are a result of quantum confinement of electrons and holes within the nanoparticle. Following the theory [23] the quantum confinement of electrons and holes in respective parabolic conduction and valence bands resulted in a ladder of energy levels $E_{l,n}$. The electron transitions between these levels can be described as:

$$\Delta E_{l,n} = E_{l,n} - E_g = \frac{\hbar^2 J_{l,n}^2}{2\mu a^2} \quad (4)$$

where $\hbar$ is Planck's constant, $J_{l,n}$ are Bessel function roots with $l = 1, 2, 3\ldots$ being the orbital quantum number and the order of Bessel function, and $n = 0, 1, 2, 3,\ldots$ being the main quantum number and the serial number of the Bessel function root; a is diameter of MeS cluster, and $\mu = \frac{m_e^* m_h^*}{m_e^* + m_h^*}$ is the reduced effective mass. From the values of $\Delta E_{l,n}$ of the de-convoluted spectra, the average diameter of nanoclusters can be found. All these data are given in Table 3. The dimensions of MeS clusters vary between 0.8 to 1.2 nm which corresponds well to the values estimated from the absorption band edges. PbS with the largest metal ion has the smallest cluster size.

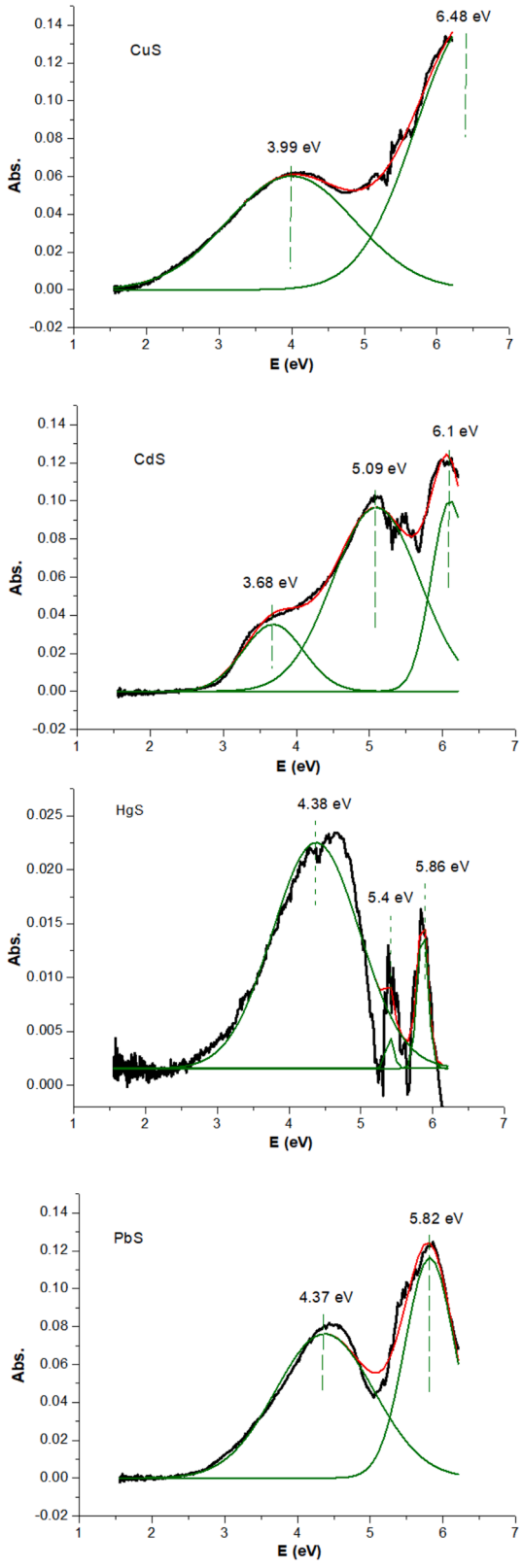

Fig. 5. Deconvolution of UV–vis spectra of metal sulfide clusters, e.g. CuS, CdS, HgS and PbS, embedded in calix(8)arene LB films (40 layers).

3.6. XPS studies

Again because of better film quality and reproducibility, we report XPS results for films deposited from salt-containing subphases. Typical XPS scans for LB films containing Cd on silicon before (a) and after (b) treatment with H_2S are shown in Fig. 6. The insets display the Cd^{3d} peaks in greater detail. Both spectra clearly show the presence of cadmium in the film and a sulfur peak appears after H_2S treatment. No peak for chlorine could be detected, indicating that cadmium ions bind solely to the carboxylic acid groups. A second band on the Cd^{3d} peak appeared as a result of H_2S treatment.

Results of the analysis of XPS spectra are summarized in Fig. 7. Columns (a) in Fig. 7 show the ratio of metal ions to calix(8)arene molecules (obtained from the areas beneath the XPS peaks for metal and carbon). The metal to carbon ratios (a) show that each calix(8)arene binds approximately 2–3 metal atoms. Lead appeared to be the most effectively adsorbed metal atom, perhaps due to high affinity for the carboxylate groups. Cadmium is also effectively adsorbed while copper and mercury display the smallest metal to calix(8)arene ratios. This is interesting since PbS displays the smallest particle size, when a simplistic view would be that higher metal levels would lead to larger particles. No Cl^- ions were detected indicating that the metal ions are present in the films as carboxylates.

Simplistically it could be expected that the metal-ion/calixarene ratio would be the same for every metal ion but results clearly show this is not the case. The interactions between metal ions and bases are often highly dependent on their relative "hardness" and "softness" [24]. Carboxylate is a relatively hard base and will bind the relatively harder Pb^{2+} ion more effectively than the other metals. However, considering its relative softness, cadmium binds very well to the LB film [25].

Initially we thought that each calix(8)arene would bind four of whatever metal salt was present and the levels of metal would be the same no matter which salt was used. Results show this not to be the case with different metals having different affinities for the carboxylate groups. This however could be an advantage since it may prove possible to tailor the resultant MeS cluster size and properties by careful control of metal ion concentrations and pH.

Columns (b) in Fig. 7 display the sulfur to metal ratios for LB films

Table 3
Energies of electron transitions between levels of size quantization and evaluation of the size of MeS clusters.

Material	ΔE_{01} (eV)	ΔE_{11} (eV)	ΔE_{21} (eV)	a (nm)
CuS	3.99	6.48		1.1 ± 0.12
CdS	3.68	5.09	6.1	1.175 ± 0.135
HgS	4.38	5.40	5.86	0.96 ± 0.11
PbS	4.37	5.82		0.784 ± 0.12

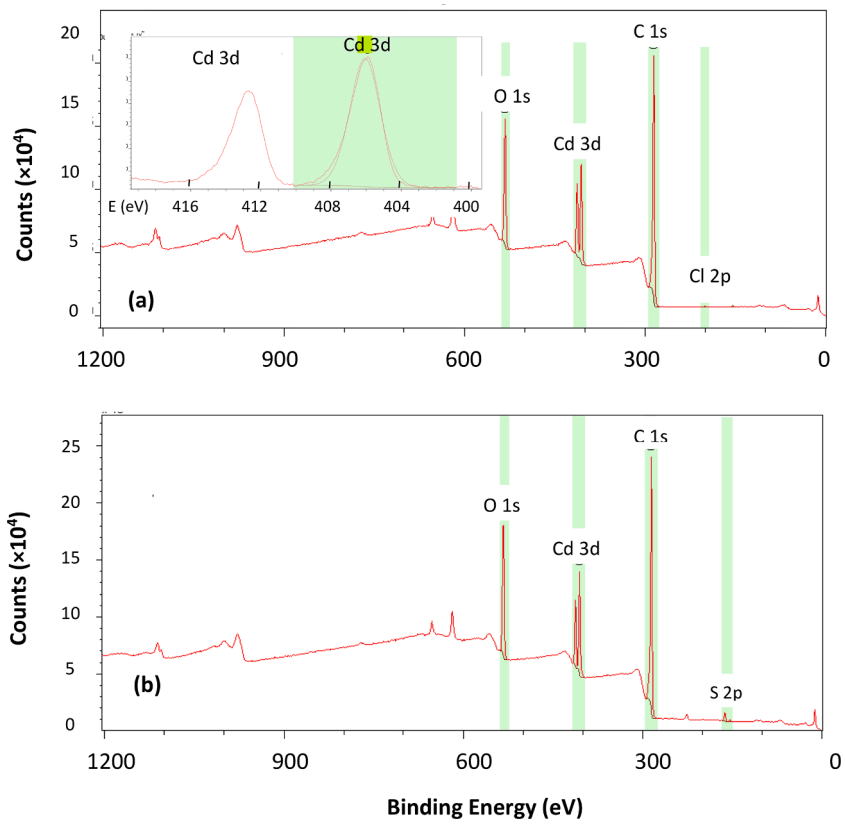

Fig. 6. Typical XPS scans for LB films (40 layers) containing Cd before (a) and after (b) treatment with H_2S. Inset shows Cd^{3d} peaks zoomed in.

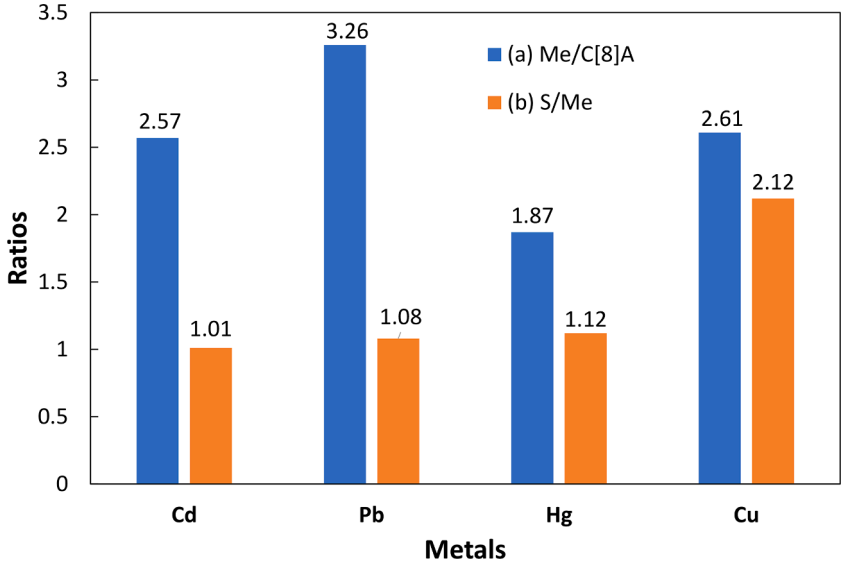

Fig. 7. Results of the XPS analysis: columns (a) show average number of metal ions per calix(8)arene molecules, columns (b) show the ratio of sulfur to metal within the films.

after treatment with H_2S. It appears that all the metal salts are converted to MeS sulfides with the exception of copper which form a species best described as CuS_2. This behavior has been previously observed for films of copper stearate [4].

4. Conclusions

Metal sulfide nano-clusters, i.e. CuS, CdS, HgS, and PbS, can be formed within LB films of calix(8)arene carboxylic acid either by adding the respective metal chloride salts in the aqueous subphase or by soaking the LB films in those salts followed by treatment in H_2S gas. The former method is more reliable and resulted in stoichiometric metal sulfides (apart from Cu which tended to form CuS_2.

UV–vis absorption spectroscopy study showed the presence of multiple absorption bands corresponding to electron transitions between energy levels in nanoclusters formed as result of quantum confinement of electrons and holes. The adsorption edges and band gaps were noticeably shifted compared to bulk metal sulfides. Two methods, the

blue shift of the adsorption edge and modeling the electronic transitions within the nanomaterials were used to determine particle sizes. Consistent results were obtained using the two techniques. The clusters obtained by this protocol are amongst the smallest obtained within LB films, being of the range 0.6–1.2 nm in size, possibly arising as a combination of restricted diffusion within the robust calix(8)arene films and a templating effect of the macrocyclic host, due to the formation of metal-calix(8)arene complexes and the subsequent formation of MeS nano-clusters within the calix(8)arene cavities. PbS gave the smallest particles, even though it had the highest levels of metal in the LB film.

There is still debate within a number of studies whether the metal sulfides exist as particles, discs or even planes within LB film composites. However, in our previous work made using TEM studies on CdS generation within calixarene films has demonstrated the formation of CdS nanoparticles [18]. Electron diffraction studies also showed the CdS to have a zinc blende type structure rather than a wurtzite type structure [18]. Also low angle X-ray diffraction studies confirmed the layer structure of the LB film and that it was retained after generation of CdS within the lattice, however in simple cadmium stearate LB films, generation of CdS destroyed the layer structure [17].

Spectroscopic ellipsometry study confirmed the formation of another substance within calix(8)arene LB films, and gave values of the film thickness consistent with calixarene dimensions. XPS data confirmed the formation of CdS, HgS, and PbS, while Cu tended to form poly-sulfides, the resultant material having the overall composition CuS_2.

Contribution of authors

Cansu Ozkaya: experimental work using LB trough, UV–vis absorption spectroscopy.

Alexei Nabok: conceptualisation, ellipsometry measurements, analysis of results, manuscript preparation and submission.

Frank Davis: conceptualisation, calixarene synthesis, preparation of chemicals, analysis of results, manuscript writing and revision.

Hisham Abu-Ali: preparation of chemicals, samples and LB trough, discussion of results.

Nik Walch: analysis of results, manuscript revision.

Deborah Hammond: XPS measurements and analysis.

Rifat Capan: conceptualisation, financial arrangement, e.g. arrangement of RASMUS-sponsored research visit of Cansu Ozkaya, discussion of results.

Acknowledgments

Ms Ozkaya would like to thank the Erasmus program for sponsoring her research visit to UK.

Declaration of Competing Interest

The authors declare the following financial interests/personal relationships which may be considered as potential competing interests:

Cansu Ozkaya reports financial support was provided by ERASMUS.

Data availability

Data will be made available on request.

References

[1] A.I. Ekimov, L. Efros, A.A. Onushchenko, Quantum size effect in semiconductormicrocrystals, Solid State Comm. 56 (1985) 921–924, https://doi.org/10.1016/S0038-1098(85)80025-9.

[2] L.E. Brus, A simple model for the ionization potential, electron affinity, and aqueous redox potentials of small semiconductor crystallites, J. Chem. Phys. 79 (1983) 5566–5571, https://doi.org/10.1063/1.445676.

[3] A.L. Ruaudel-Teixier, J. Leloup, A.I. Barraud, Insertion compounds in L.B. films, Mol. Cryst. Liq. Cryst. 134 (1986) 347–354, https://doi.org/10.1080/00268948608079595.

[4] H. Chen, X. Chai, Q. Wei, Y. Jiang, T. Li, X-ray photoelectron spectroscopy study of the synthesis of copper sulphide in Langmuir-Blodgett films, Thin Solid Films 178 (1989) 535–540, https://doi.org/10.1016/0040-6090(89)90349-0.

[5] C. Zylberajch, A. Ruaudel-Teixier, A. Barraud, 2D monomolecular inorganic semiconductors, inserted in a Langmuir-Blodgett matrix, Synth. Met. 27 (1988) B609–B614, https://doi.org/10.1016/0379-6779(88)90207-X.

[6] E.S. Smotkin, C. Lee, A.J. Bard, A. Campion, M.A. Fox, T.M. Mallouk, S.E. Webber, J.M. White, Size quantization effects in cadmium sulfide layers formed by a Langmuir-Blodgett technique, Chem. Phys. Lett. 152 (1988) 265–268, https://doi.org/10.1016/0009-2614(88)87365-2.

[7] I. Moriguchi, I. Tanaka, Y. Teraoka, S. Kagawa, Production and growth of size-quantized cadmium sulphide in the hydrophilic interlayer of Langmuir–Blodgett films, J. Chem. Soc., Chem. Commun. (1991) 1401–1402, https://doi.org/10.1039/C39910001401.

[8] I. Moriguichi, K. Hosoi, H. Nagaoka, I. Tanaka, Y. Teraoka, S. Kagawa, Stepwise growth of size-confined CdS in the two-dimensional hydrophilic interlayers of Langmuir–Blodgett films by the repeated sulfidation–intercalation technique, J. Chem. Soc. Faraday Trans. 90 (1994) 349–354, https://doi.org/10.1039/FT9949000349.

[9] F. Grieser, D.N. Furlong, D. Scoberg, I. Ichinose, N. Kimizuka, T. Kunitake, Size-quantised semiconductor cadmium chalcogenide particles in Langmuir–Blodgett films, J. Chem. Soc. Faraday Trans. 88 (1992) 2207–2214, https://doi.org/10.1039/FT9928802207.

[10] M. Isamu, S. Futoshi, Y. Yasutake, K. Shuichi, Control of size of CdS formed in organized molecular assembly films by molecular structure and film orderliness, Chem. Lett. 24 (24) (1995) 761–762, https://doi.org/10.1246/cl.1995.761.

[11] I. Moriguchi, H. Nii, K. Hanai, H. Nagaoka, Y. Teraoka, S. Kagawa, Synthesis of size-confined metal sulfides in Langmuir-Blodgett films, Coll. Surf. A. 103 (1995) 173–181, https://doi.org/10.1016/0927-7757(95)03238-9.

[12] I. Moriguchi, K, M. Matsuo, K. Sakai, Y.T. Hanai, S. Kagawa, Synthesis of size-quantized metal sulfides of Pb–Cd and Zn–Cd bimetallic systems in stearate Langmuir–Blodgett films, J. Chem. Soc. Faraday Trans. 94 (1998) 2199–2204, https://doi.org/10.1039/A801910J.

[13] A. Hiisselbart, A. Eychmuller, R. Eicbberger, M. Giersig, A. Mews, H. Weller, Preparation, characterization, and photophysics of the quantum dot quantum well system cadmium sulfide/mercury sulfide/cadmium sulfide, J. Phys. Chem. 98 (1994) 934–941, https://doi.org/10.1021/J100054A032.

[14] T. Richardson, M.B. Greenwood, F. Davis, C.J.M. Stirling, Calix(8)arene LB superlattices: pyroelectric molecular baskets, IEE Proc. Circ. Dev. Syst. 144 (1997) 108–110, 10.1049/ip-cds:19971027.

[15] Z. Ali-Adib, Davis F, P. Hodge, C.J.M. Stirling, Structures and binding of LB films of calix-8-arenes, Supramol. Sci. 4 (1997) 201–206, https://doi.org/10.1016/S0968-5677(97)00005-9.

[16] A.V. Nabok, T. Richardson, F. Davis, C.J.M. Stirling, Cadmium sulfide nanoparticles in Langmuir−Blodgett films of calixarenes, Langmuir 13 (1997) 3198–3201, https://doi.org/10.1021/LA962115F.

[17] A.V. Nabok, T. Richardson, C. McCartney, N. Cowlam, F. Davis, C.J.M. Stirling, V. Gacem, A. Gibaud, Size-quantization in extremely small CdS clusters formed in calixarene LB films, Thin Solid Films 327 (9) (1998) 510–514, https://doi.org/10.1016/S0040-6090(98)00699-3.

[18] A.V. Nabok, A. Ray, A.K. Hassan, A.J. Titchmarsh, F. Davis, T. Richardson, A. Starovoitov, S. Bayliss, Formation of CdS nanoclusters within LB films of calixarene derivatives and study of their size-quantization, Mater. Sci. Eng. C8-C9 (1999) 171–177, https://doi.org/10.1016/S0928-4931%2899%2900012-0.

[19] K. Przykaza, K. Woźniak, M. Jurak, A.E. Wiącek, R. Mroczka, Properties of the Langmuir and Langmuir–Blodgett monolayers of cholesterolcyclosporine A on water and polymer support, Adsorption 25 (2019) 923–936, https://doi.org/10.1007/s10450-019-00117-2.

[20] T. Richardson, M.B. Greenwood, F. Davis, C.J.M. Stirling, Pyroelectric molecular baskets: temperature-dependent polarization from substituted Calix(8)arene Langmuir- Blodgett Films, Langmuir 11 (1995) 4623–4625, https://doi.org/10.1021/la00012a006.

[21] I.M. Lifshiz, V.V. Slezov, Kinetics of diffusive decomposition of supersaturated solid solutions, Sov. Phys. JETP 35 (8) (1959) 331–339. Journal of Experimental and Theoretical Physics (jetp.ras.ru).

[22] J.M. Harrowfield, M.1. Ogden, W.R. Richmond, A.H. White, Calixarene-cupped caesium: a coordination conundrum? J. Chem. Soc. Chem. Commun. (1991) 1159–1161, https://doi.org/10.1039/C39910001159.

[23] A.I. Ekimov, A.L. Efros, A.A. Onushenko, Quantum size effect in semiconductor microcrystals, Solid State. Comm. 88 (1993) 947–950, https://doi.org/10.1016/0038-1098(93)90275-R.

[24] R.G. Pearson, Hard and soft acids and bases, J. Am. Chem. Soc. 85 (1963) 3533–3539, https://doi.org/10.1021/ja00905a001.

[25] H. Xu, D.C. Xu, Y. Wang, Natural indices for the chemical hardness/softness of metal cations and ligands, ACS Omega 2 (2017) 7185–7193, https://doi.org/10.1021/acsomega.7b01039.